Photon Lasers Med 1 (2012): 35–40 © 2012 by Walter de Gruyter • Berlin • Boston. DOI 10.1515/plm-2011-0011

Review

Multidimensional fluorescence microscopy in live cell imaging – A mini review

Bildgebende multidimensionale Fluoreszenzmikroskopie an lebenden Zellen

Herbert Schneckenburger[1,2,*], Petra Weber[1], Michael Wagner[1], Thomas Bruns[1], Verena Richter[1], Sarah Schickinger[1] and Rainer Wittig[2]

[1] Institut für Angewandte Forschung, Hochschule Aalen, Beethovenstrasse 1, 73430 Aalen, Germany, e-mail: herbert.schneckenburger@htw-aalen.de
[2] Institut für Lasertechnologien in der Medizin und Messtechnik an der Universität Ulm, Helmholtzstrasse 12, 89081 Ulm, Germany

* Corresponding author

Abstract

Fluorescence microscopy methods are described with high spatial, spectral, and temporal resolution. In addition to three-dimensional (3D) microscopy, based on confocal, structured, or single-plane illumination, spectral imaging and fluorescence lifetime imaging microscopy are used to probe the conformation of fluorescent molecules as well as their interaction with the microenvironment. In addition to single cells or cell monolayers, 3D cell cultures are used increasingly, as they are more representative for tissue morphology and function. All methods are discussed in the context of controlled light exposure, which is regarded as a key parameter to maintain cell viability. The applications presented in this mini review include autofluorescence measurements of glioblastoma cells as well as various fluorescent markers or fluorescent proteins.

Keywords: living cells; confocal microscopy; structured illumination; SPIM; spectral imaging; FLIM; autofluorescence; light dose.

Zusammenfassung

Fluoreszenzmikroskopische Methoden mit hoher räumlicher, spektraler und zeitlicher Auflösung werden beschrieben. Neben der 3D-Mikroskopie mit konfokaler oder strukturierter Beleuchtung sowie der Lichtscheibenmikroskopie wird die spektral und zeitlich hoch auflösende Bildgebung benutzt, um die Konformation fluoreszierender Moleküle sowie deren Wechselwirkung mit der Mikroumgebung zu untersuchen. Zusätzlich zu Einzelzellen oder Zell-Monolayern werden in zunehmendem Maße drei-dimensionale Zellkulturen verwendet, die Morphologie und Funktion der Gewebe besser repräsentieren. Alle vorgestellten Methoden werden im Hinblick auf deren Lichtbelastung diskutiert, die für die Erhaltung der Zellvitalität wesentlich ist. Die vorgestellten Anwendungen umfassen Autofluoreszenzmessungen von Glioblastomzellen sowie verschiedene Fluoreszenzmarker und fluoreszierende Proteine.

Schlüsselwörter: Lebende Zellen; Konfokale Mikroskopie; Strukturierte Beleuchtung; Lichtscheibenmikroskopie; Spektrale Bildgebung; FLIM; Autofluoreszenz; Lichtdosis.

1. Introduction

Spatial resolution is a key parameter in modern fluorescence microscopy. As light diffraction often limits lateral as well as axial resolution, further restrictions are due to a low focal depth when an image from the focal plane is superposed by out-of-focus contributions. This plays a predominant role if conventional two-dimensional (2D) samples, e.g., cell cultures growing on a glass slide, are replaced by three-dimensional (3D) systems, e.g., cell spheroids (Figure 1) or tissue samples. Therefore, methods of optical sectioning are required where information from individual planes is selected and possibly combined in a high-resolution 3D image. Those techniques include laser scanning microscopy (LSM) as well as wide-field microscopy with structured or single-plane illumination as is described in the present paper.

In multidimensional microscopy, spatial resolution is often combined with high spectral or temporal resolution, thus resulting in spectral imaging or fluorescence lifetime imaging microscopy (FLIM). In addition to precise localization of fluorescent probes, these techniques often allow the measurement of intermolecular interactions with their microenvironment. Non-radiative (Förster resonance) energy transfer (FRET) from a donor to an acceptor molecule [1] plays an important role in this context, as intermolecular distances below 10 nm can be detected reliably.

With increasing magnification, illuminated areas in a microscope become progressively smaller, and power densities often exceed solar irradiance of about 100 mW/cm^2 (corresponding to 1 nW/μm^2), which is used as a reference value. This may cause damage to living cells, and requires alternative methods of low light exposure. The present article summarizes methods

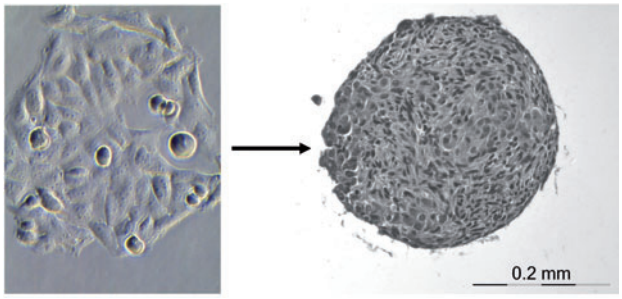

Figure 1 Substitution of 2D cell monolayers by 3D spheroids, which are more similar to tissue morphology and function (here U373-MG glioblastoma cells).

of fluorescence microscopy permitting low light doses and describes some applications with cultivated glioblastoma cells, grown either as monolayers on glass slides [2] or as 3D spheroids of about 300 µm diameter [3].

2. Laser scanning microscopy

More than 25 years ago, confocal LSM was introduced as a promising method for 3D microscopy with high axial resolution [4, 5]. This method is based on scanning a sample with a focused laser beam and imaging each spot of the sample on a confocal pinhole. This allows an image from the focal plane to be selected and light from out-of-focus planes to be excluded. Shifting the sample in an axial direction allows a larger number of planes to be imaged and full 3D information to be obtained.

Resolution is determined by light diffraction – dependent on the numerical aperture (NA) of the objective lens – and typically varies between 200 nm (lateral) as well as 350 nm (axial) for a 100×/1.45 high-aperture lens and about 1 µm (lateral) as well as 6 µm (axial) for a 10×/0.30 low aperture lens. High resolution in the first case is suitable for subcellular imaging, whereas lower resolution in the second case may be appropriate to select, e.g., a single cell layer from a larger 3D sample. An example for this latter case is given in Figure 2, where confocal images from various planes of a spheroid of U373-MG glioblastoma cells incubated with the fluorescent marker acridine orange are depicted, which may be further used to calculate a 3D image of the sample.

Numerous modifications of LSM have in the meantime been developed. In two-photon or multiphoton microscopy [6, 7], fluorescence arises from simultaneous absorption of two or several photons by the same molecule in the picosecond to femtosecond time range. Since multiphoton excitation is restricted to the focus of the laser beam, an image is created only from the focal plane and no pinhole is needed in the detection path. A further advantage of multiphoton microscopy is that fluorescence in the whole visible spectral range can be excited by red or near-infrared light with a larger penetration depth in scattering samples. The principal disadvantage of a longer wavelength, and therefore lower resolution, can be compensated for by further methods limiting the excitation volume, e.g., 4Pi microscopy [8, 9] or standing wave microscopy [8].

As a method with extremely high resolution, stimulated emission depletion (STED) microscopy is described as a Gaussian laser beam exciting the sample and an additional ring-shaped (donut) beam causing stimulated emission and preventing the sample from fluorescence, except from a very tiny central part [10]. This permits a lateral resolution down to about 30 nm but requires laser powers of several hundred milliwatts focused to a scanned area of about 100×100 µm.

3. Wide-field microscopy

In contrast to LSM, wide-field microscopy allows observation of larger areas of the sample. Here, selective imaging of a focal plane and discrimination of out-of-focus light requires special techniques, some of which are described in the following sections.

3.1. Structured illumination

Structured illumination is performed by projection of an optical pattern into different positions of a sample. For example, a grid can be imaged into the sample plane at three different phase angles. From these structured images, an unstructured image from the focal plane is easily calculated by a

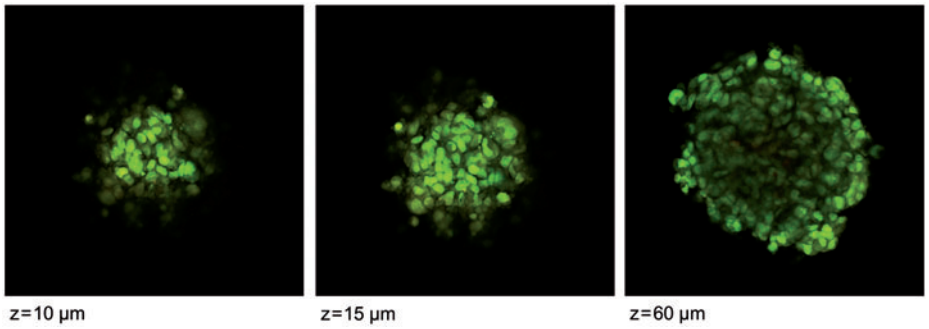

Figure 2 Focal planes of a spheroid of U373-MG glioblastoma cells incubated with acridine orange (5 µM; 40 min) at different distances z from top of the sphere (confocal fluorescence microscopy; excitation wavelength, 488 nm; fluorescence detection, ≥505 nm; image size, 460×460 µm).

mathematical algorithm [11], whereas out-of-focus parts of the image vanish completely. Axial resolution again depends on the NA of the objective lens as well as on the spatial frequency of the grid and may attain values below 1 µm. In an improved setup with a 3D interference structure, values of even 100 nm of lateral resolution and 200 nm of axial resolution have been attained [12]. However, in larger samples (e.g., cell spheroids), selection of individual cell layers with 5–10 µm diameter may be more important than subcellular resolution. Therefore, a modular system was recently developed [13], where an optical grid with 10 line pairs per millimeter is imaged on the sample by an objective lens of moderate magnification (5–20×) and NA (0.15–0.50). Large image fields from various axial positions (used for 3D reconstruction), exchangeable light sources (e.g., LEDs), and low light exposure are the main advantages of this setup.

3.2. Single-plane illumination microscopy

An inherent disadvantage of both LSM and structured illumination microscopy is that when recording each plane, the whole sample is exposed to light. Therefore, in 3D imaging, the light dosage adds up over numerous single-plane experiments and phototoxic damage can easily occur. This problem can be overcome by single-plane illumination microscopy (SPIM) [14, 15], where the sample is illuminated by a light sheet in a perpendicular direction to the observation path. This light sheet can be generated with a typical diameter of 1–10 µm by a cylindrical lens or by scanning a laser beam. Thus, only those planes are exposed to light, which are examined simultaneously, and even upon successive measurements of multiple planes, light exposure of the whole sample is comparable to that of a single-plane experiment. This permits prolonged exposure times in 3D imaging or during kinetic measurements.

3.3. Variable-angle total internal reflection microscopy

Sample surfaces can be illuminated selectively by an evanescent electromagnetic field arising from total internal reflection (TIR) of a laser beam on a cell-substrate interface [16]. Axial resolution is generally given by the penetration depth of the evanescent wave, which depends on the angle of incidence and varies between about 70 and 200 nm. This resolution can be used for many studies of cell membranes related to accumulation of specific markers, exocytosis or endocytosis, or transmembrane ion fluxes (for a review, see [17]). A layer of about 100 nm diameter is also sufficient for single-molecule experiments [18] used in superlocalization microscopy, e.g., stochastic optical resolution microscopy (STORM) or photoactivated localization microscopy (PALM) [19–21]. However, axial resolution can be further lowered if fluorescence intensity, I_F, is determined as a function of the angle of incidence, Θ, over a range of 6–10° [22]. In this case, cell-substrate topology is measured with nanometer precision, as was recently reported for cell adhesion dependent on the amount of cholesterol or on photodynamic laser treatment [23].

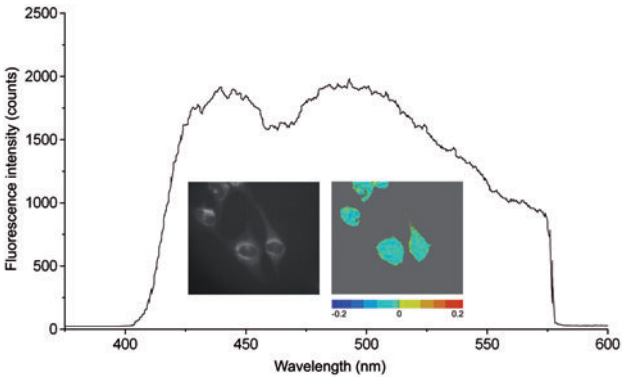

Figure 3 Emission spectrum of intrinsic fluorescence of U251-MG glioblastoma cells (excitation wavelength, 375 nm); inlay: fluorescence intensity (left) and PBP with scale (right) of NADH; image size, 140×140 µm.

4. Microspectral imaging

Microspectral imaging combines spatial and spectral resolution in microscopy by insertion of dispersive elements, e.g., gratings, filters, interferometric devices (for a review, see [24]). This allows information to be gained about fluorescent molecules, e.g., their conformation or intermolecular interactions. It is well known that the coenzyme nicotinamide adenine dinucleotide (NADH), which plays a predominant role in cell metabolism (respiration as well as anaerobic glycolysis), occurs both in a folded and in an extended conformation, dependent on whether this molecule is free or bound to proteins [25, 26]. Both species have broad fluorescence bands with maxima at 470–480 and 440 nm, respectively, which dominate the emission spectrum of many cell types upon excitation at 340–380 nm (Figure 3). Use of broad band interference filters, e.g., 450±20 and 490±20 nm, allows a rather selective measurement of these components and definition of a protein binding parameter (PBP)=$(I_{450}$-$I_{490})$/$(I_{450}$+$I_{490})$ [2]. This parameter is depicted in the inlay of Figure 3 and shows less protein binding of NADH in some fluorescent granules surrounding the cell nucleus than in other parts of the cells, possibly due to a difference in the cell metabolism. Further applications of spectral imaging, e.g., imaging of membrane stiffness with polarity-sensitive fluorescent markers [27] or imaging of intermolecular energy transfer (FRET) – with a large spectrum of applications (see, e.g., [28, 29]) – are well documented in the literature.

5. Fluorescence lifetime imaging microscopy

The fluorescence lifetime corresponds to the reciprocal of all rates of deactivation of an excited molecular state – including fluorescence (k_F), internal conversion (k_{IC}), intersystem crossing (k_{ISC}), and non-radiative intermolecular energy transfer (k_{ET}). As some of these rates (k_{IC}, k_{ET}) are rather sensitive to molecular conformation, aggregation, or intermolecular interactions, fluorescence lifetime has become a very sensitive parameter for these mechanisms.

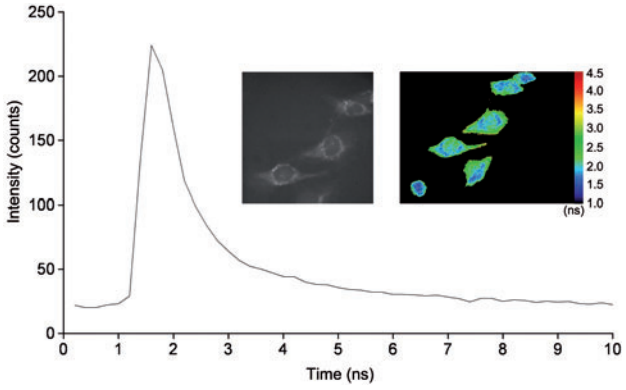

Figure 4 Fluorescence decay curve of intrinsic fluorescence of U251-MG glioblastoma cells (excitation wavelength, 375 nm); inlay: fluorescence intensity (left) and effective lifetime (right); image size, 140×140 µm (left) and 160×220 µm (right).

Over the last 10 years, FLIM has become a well-established technique. LSM with time-correlated single-photon counting [30] and ultrafast camera technology [31, 32] are currently used. An example is given in Figure 4, where the fluorescence decay curve of a single human glioblastoma cell is depicted. This curve represents a biexponential decay with fluorescence lifetimes of τ_1=0.4–0.5 ns and τ_2=2.3–2.8 ns corresponding to free and protein-bound NADH, respectively. If instead of individual fluorescence lifetimes, the so-called effective lifetime (τ_{eff}, which would result from monoexponential curve fitting) is evaluated, a fluorescence lifetime image results as is depicted in the inlay of Figure 4. This image shows lower effective lifetimes in the granules surrounding the cell nucleus than in other parts of the cells and again indicates a higher amount of free NADH in these granules. Measurements on cells of different malignancy [2] show a decrease in fluorescence lifetimes with increasing malignancy, thereby indicating differences in cell metabolism.

FLIM is an ideal method for proving FRET between adjacent molecules. Recent applications include sensing of calcium metabolism [33] or apoptosis [34, 35] as well as studies of pathogenesis of various diseases (e.g., cancer [36], Alzheimer disease [37]).

6. Light dose in microscopy

In general, in microscopy, light of moderate intensity is focused on small areas, resulting in power densities that often considerably exceed solar irradiance of 100 mW/cm^2. Although this problem is well known, phototoxic cell damage has so far only been addressed by a few articles [38–40]. Recently, maximum light doses of 25–200 J/cm^2 (corresponding to 250–2000 s of solar irradiance and increasing with the excitation wavelength from 375 to 633 nm) have been found to be nonphototoxic toward native U373-MG glioblastoma cells [40]. These tolerable light doses increased by about a factor of 3 when cells were illuminated by an evanescent electromagnetic field arising from TIR but decreased when incubated with fluorescent markers or transfection with plasmids encoding for fluorescent proteins [41].

So far, the highest light doses are needed for some methods of super-resolution or superlocalization microscopy. Methods based on single molecule detection (e.g., PALM, STORM) require about 50–100 W/cm^2 (corresponding to 5–10 mW on a sample area of 0.01 mm^2) to record typically 100 fluorescence photons per second from one molecule. Assuming that the maximum tolerable light dose from TIR illumination is 300–600 J/cm^2, exposure times should be therefore limited to a few seconds. Irradiance in STED microscopy is even higher (about 10,000–100,000 solar constants), when a laser power of a few hundred milliwatts [10] is used to scan an object field of about 0.01 mm^2. In this case, it is impossible to specify any tolerable exposure time.

Conventional wide-field microscopy or LSM can be performed with solar irradiance, when a power of about 10 µW is applied to a surface of 0.01 mm^2. In this case, native cells can be illuminated for up to 250–2000 s and cells incubated with a fluorescent marker for up to about 10–500 s, dependent on the fluorophore, its concentration, and excitation wavelength [41]. This permits, for example, recording of several planes of a sample by LSM or structured illumination microscopy needed to obtain a 3D image. At a lower magnification (as was used for the cell spheroids reported previously), irradiance may be reduced and larger exposure times become possible. This is the case for SPIM in particular, where – in contrast to all other methods with axial resolution – each plane of the sample is illuminated only once. Therefore, SPIM appears to be an ideal method for 3D microscopy of larger samples, even with rather long exposure times.

7. Concluding remarks

In summary, numerous methods have been described to obtain high 3D resolution in microscopy. These methods can be combined with temporal or spectral resolution to obtain additional information on molecular conformation or aggregation of fluorophores as well as on interaction with their microenvironment. Phototoxicity toward living cells may play some major role in high-resolution or super-resolution microscopy, and limitation of the integral light dose appears to be cogent. A promising approach toward lower light doses seems to be controlled light exposure microscopy [38, 42], where the excitation light is adapted to the local concentration of fluorophores. In particular, using an electronic feedback system, illumination is reduced in regions of high fluorescence as well in the background of the image. Therefore, phototoxicity and photobleaching are minimized without affecting the image quality. Finally, it should be emphasized that cell viability in nonlinear, e.g., multiphoton microscopy has not been addressed by the present article.

Acknowledgements

The present mini review includes some work of the authors, who thank the Land Baden-Württemberg and the Europäische Union – Europäischer Fonds für die regionale Entwicklung for funding the ZAFH-PHOTON^n, the Bundesministerium für Bildung und Forschung (BMBF) for funding research grant 1792C08, and the Baden-Württemberg-Stiftung gGmbH for financing the project "Aurami".

References

[1] Förster T. Zwischenmolekulare Energiewanderung und Fluoreszenz. Ann Physik 1948;6(2):55–75.
[2] Schneckenburger H, Weber P, Wagner M, Brantsch M, Biller P, Kioschis P, Kessler W. Tumor cell differentiation by marker free fluorescence microscopy. Proc SPIE 2011;7902:79020D.
[3] Schneckenburger H, Wagner M, Weber P, Bruns T, Richter V, Strauss WS, Wittig R. Multi-dimensional fluorescence microscopy of living cells. J Biophotonics 2011;4(3):143–9.
[4] Pawley J. Handbook of biological confocal microscopy. New York: Plenum Press; 1990.
[5] Webb RH, Confocal optical microscopy. Rep Prog Phys 1996;59(3):427–71.
[6] Denk W, Strickler JH, Webb WW. Two-photon laser scanning fluorescence microscopy. Science 1990;248(4951):73–6.
[7] König K. Multiphoton microscopy in life sciences. J Microsc 2000;200(Pt 2):83–104.
[8] Gustafsson MG. Extended resolution fluorescence microscopy. Curr Opin Struct Biol 1999;9(5):627–34.
[9] Martini N, Bewersdorf J, Hell SW. A new high-aperture glycerol immersion objective lens and its application to 3D-fluorescence microscopy. J Microsc 2002;206(Pt 2):146–51.
[10] Willig KI, Harke B, Medda R, Hell SW. STED microscopy with continuous wave beams. Nat Methods 2007;4(11):915–8.
[11] Neil MA, Juskaitis R, Wilson T. Method of obtaining optical sectioning by using structured light in a conventional microscope. Opt Lett 1997;22(24):1905–7.
[12] Gustafsson MG, Shao L, Carlton PM, Wang CJ, Golubovskaya IN, Cande WZ, Agard DA, Sedat JW. Three-dimensional resolution doubling in wide-field fluorescence microscopy by structured illumination. Biophys J 2008;94(12):4957–70.
[13] Richter V, Bruns T, Weber P, Strauss WSL, Wittig R, Schneckenburger H. 3D fluorescence imaging of tumor cell spheroids. Proc SPIE 2011;8089:80890D.
[14] Huisken J, Swoger J, Del Bene F, Wittbrodt J, Stelzer EH. Optical sectioning deep inside live embryos by selective plane illumination microscopy. Science 2004;305(5686):1007–9.
[15] Santi PA. Light sheet fluorescence microscopy: a review. J Histochem Cytochem 2011;59(2):129–38.
[16] Axelrod D. Cell-substrate contacts illuminated by total internal reflection fluorescence. J Cell Biol 1981;89(1):141–5.
[17] Schneckenburger H. Total internal reflection fluorescence microscopy: technical innovations and novel applications. Curr Opin Biotechnol 2005;16(1):13–8.
[18] Sako Y, Uyemura T. Total internal reflection fluorescence microscopy for single-molecule imaging in living cells. Cell Struct Funct 2002;27(5):357–65.
[19] Betzig E, Patterson GH, Sougrat R, Lindwasser OW, Olenych S, Bonifacino JS, Davidson MW, Lippincott-Schwartz J, Hess HF. Imaging intracellular fluorescent proteins at nanometer resolution. Science 2006;313(5793):1642–5.
[20] Rust MJ, Bates M, Zhuang X. Sub-diffraction-limit imaging by stochastic optical reconstruction microscopy (STORM). Nat Methods 2006;3(10):793–5.
[21] Hess ST, Girirajan TP, Mason MD. Ultra-high resolution imaging by fluorescence photoactivation localization microscopy. Biophys J 2006;91(11):4258–72.
[22] Stock K, Sailer R, Strauss WS, Lyttek M, Steiner R, Schneckenburger H. Variable-angle total internal reflection fluorescence microscopy (VA-TIRFM): realization and application of a compact illumination device. J Microsc 2003;211(Pt 1):19–29.
[23] Wagner M, Weber P, Strauss WSL, Lassalle H-P, Schneckenburger H. Nanotomography of cell surfaces with evanescent fields. Adv Opt Technol 2008; 2008:254317:1–7. doi:10.1155/2008/254317.
[24] Garini Y, Young IT, McNamara G. Spectral imaging: principles and applications. Cytometry A 2006;69(8):735–47.
[25] Salmon JM, Kohen E, Viallet P, Hirschberg JG, Wouters AW, Kohen C, Thorell B. Microspectrofluorometric approach to the study of free/bound NAD(P)H ratio as metabolic indicator in various cell types. Photochem Photobiol 1982;36(5):585–93.
[26] Skala MC, Riching KM, Gendron-Fitzpatrick A, Eickhoff J, Eliceiri KW, White JG, Ramanujam N. In vivo multiphoton microscopy of NADH and FAD redox states, fluorescence lifetimes, and cellular morphology in precancerous epithelia. Proc Natl Acad Sci USA 2007;104(49):19494–9.
[27] Weber P, Wagner M, Schneckenburger H. Fluorescence imaging of membrane dynamics in living cells. J Biomed Opt 2010;15(4):046017.
[28] Hanley QS, Murray PI, Forde TS. Microspectroscopic fluorescence analysis with prism-based imaging spectrometers: review and current studies. Cytometry A 2006;69(8):759–66.
[29] Sun Y, Wallrabe H, Booker CF, Day RN, Periasamy A. Three-color spectral FRET microscopy localizes three interacting proteins in living cells. Biophys J 2010;99(4):1274–83.
[30] Becker W. Advanced time-correlated single photon counting techniques. Berlin, Heidelberg: Springer; 2005.
[31] Cole MJ, Siegel J, Webb SE, Jones R, Dowling K, Dayel MJ, Parsons-Karavassilis D, French PM, Lever MJ, Sucharov LO, Neil MA, Juskaitis R, Wilson T. Time-domain whole-field fluorescence lifetime imaging with optical sectioning. J Microsc 2001;203(Pt 3):246–57.
[32] Li DD, Arlt J, Tyndall D, Walker R, Richardson J, Stoppa D, Charbon E, Henderson RK. Video-rate fluorescence lifetime imaging camera with CMOS single-photon avalanche diode arrays and high-speed imaging algorithm. J Biomed Opt 2011;16(9):096012.
[33] Brasselet S, Peterman EJG, Miyawaki A, Moerner WE. Single-molecule fluorescence resonant energy transfer in calcium concentration dependent cameleon. J Phys Chem B 2000;104(15):3676–82.
[34] Mahajan NP, Harrison-Shostak DC, Michaux J, Herman B. Novel mutant green fluorescent protein protease substrates reveal the activation of specific caspases during apoptosis. Chem Biol 1999;6(6):401–9.
[35] Angres B, Steuer H, Weber P, Wagner M, Schneckenburger H. A membrane-bound FRET-based caspase sensor for detection of apoptosis using fluorescence lifetime and total internal reflection microscopy. Cytometry A 2009;75(5):420–7.
[36] Lu S, Wang Y. Fluorescence resonance energy transfer biosensors for cancer detection and evaluation of drug efficacy. Clin Cancer Res 2010;16(15):3822–4.

[37] von Arnim CA, von Einem B, Weber P, Wagner M, Schwanzar D, Spoelgen R, Strauss WL, Schneckenburger H. Impact of cholesterol level upon APP and BACE proximity and APP cleavage. Biochem Biophys Res Commun 2008;370(2):207–12.

[38] Hoebe RA, Van Oven CH, Gadella TW Jr, Dhonukshe PB, Van Noorden CJ, Manders EM. Controlled light-exposure microscopy reduces photobleaching and phototoxicity in fluorescence live-cell imaging. Nat Biotechnol 2007;25(2):249–53.

[39] Frigault MM, Lacoste J, Swift JL, Brown CM. Live-cell microscopy – tips and tools. J Cell Sci 2009;122(Pt 6):753–67.

[40] Wagner M, Weber P, Bruns T, Strauss WS, Wittig R, Schneckenburger H. Light dose is a limiting factor to maintain cell viability in fluorescence microscopy and single molecule detection. Int J Mol Sci 2010;11(3):956–66.

[41] Schneckenburger H, Weber P, Wagner M, Schickinger S, Richter V, Bruns T, Strauss WS, Wittig R. Light exposure and cell viability in fluorescence microscopy. J Microsc 2011. doi: 10.1111/j.1365-2818.2011.03576.x.

[42] De Vos WH, Hoebe RA, Joss GH, Haffmans W, Baatout S, Van Oostveldt P, Manders EM. Controlled light exposure microscopy reveals dynamic telomere microterritories throughout the cell cycle. Cytometry A 2009;75(5):428–39.

Received May 11, 2011; revised September 30, 2011; accepted October 19, 2011